Published online 21 March 2021

Nucleic Acids Research, 2021, Vol. 49, No. 7 ***3997–4007***
doi: 10.1093/nar/gkab138

Iron–sulfur biology invades tRNA modification: the case of U34 sulfuration

Jingjing Zhou[1,†], Marine Lénon[2,†], Jean-Luc Ravanat[3], Nadia Touati[4], Christophe Velours[5], Karolina Podskoczyj[6], Grazyna Leszczynska[6], Marc Fontecave[1], Frédéric Barras[2,*] and Béatrice Golinelli-Pimpaneau[1,*]

[1]Laboratoire de Chimie des Processus Biologiques, UMR 8229 CNRS, Collège de France, Sorbonne Universités, 11 Place Marcelin Berthelot, 75231 Paris cedex 05, France, [2]Department of Microbiology, Stress Adaptation and Metabolism in Enterobacteria Unit, UMR CNRS 2001, Institut Pasteur, 25–28 Rue du Dr Roux, 75015 Paris, France, [3]University of Grenoble Alpes, CEA, CNRS, IRIG, SyMMES, UMR 5819, F-38000 Grenoble, France, [4]IR CNRS Renard, Chimie-ParisTech, 11 rue Pierre et Marie Curie, 75005 Paris, France, [5]Institute for Integrative Biology of the Cell (I2BC), CEA, CNRS, Université Paris-Saclay, Avenue de la Terrasse, 91198 Gif-sur-Yvette cedex, France and [6]Institute of Organic Chemistry, Faculty of Chemistry, Lodz University of Technology, Zeromskiego 116, 90-924 Lodz, Poland

Received November 02, 2020; Revised February 17, 2021; Editorial Decision February 18, 2021; Accepted February 19, 2021

ABSTRACT

Sulfuration of uridine 34 in the anticodon of tRNAs is conserved in the three domains of life, guaranteeing fidelity of protein translation. In eubacteria, it is catalyzed by MnmA-type enzymes, which were previously concluded not to depend on an iron–sulfur [Fe–S] cluster. However, we report here spectroscopic and iron/sulfur analysis, as well as *in vitro* catalytic assays and site-directed mutagenesis studies unambiguously showing that MnmA from *Escherichia coli* can bind a [4Fe–4S] cluster, which is essential for sulfuration of U34-tRNA. We propose that the cluster serves to bind and activate hydrosulfide for nucleophilic attack on the adenylated nucleoside. Intriguingly, we found that *E. coli* cells retain s^2U34 biosynthesis in the Δ*iscUA* Δ*sufABCDSE* strain, lacking functional ISC and SUF [Fe–S] cluster assembly machineries, thus suggesting an original and yet undescribed way of maturation of MnmA. Moreover, we report genetic analysis showing the importance of MnmA for sustaining oxidative stress.

INTRODUCTION

Transfer RNAs (tRNAs) are essential components of the cellular translation machinery in the three domains of life. To achieve their function, these molecules feature a great variety of well-conserved post-transcriptional chemical modifications (1–3). In particular, sulfuration of uridine 34 (Figure 1A) at the wobble position of the anticodon in glutamate-, glutamine- and lysine-tRNA is conserved in bacteria, archaea and eukaryotes and guarantees fidelity of protein translation (4,5).

U34-tRNA sulfuration is catalyzed by MnmA-type enzymes in bacteria (6–8) and mitochondria (9), and by Ncs6-type enzymes in archaea and the eukaryotic cytosol (10–12). MnmA belongs to the minimal set of proteins that can sustain translation of the genetic code in *Mollicutes* (13), a lineage of the bacterial Firmicutes that has evolved by massive genome reduction. Mutations in the *mnmA* gene resulted in severe growth reduction in *Escherichia coli* (6,14) and *Salmonella enterica* serovar Typhimurium (15,16) and in nonviability in *Bacillus subtilis* (17). Altogether, these observations support both the key role of bacterial MnmA and its probable ancient origin.

MnmA from *E. coli* belongs to a sulfur relay pathway involving multiple proteins (18): IscS, a cysteine desulfurase that abstracts the sulfur atom from L-cysteine and transfers it via trans-persulfuration reactions onto a series of various sulfur carriers; TusA, a TusBCD complex; and TusE, which eventually interacts with the MnmA–tRNA complex (7). It was proposed that sulfur would be transferred from one conserved cysteine residue of TusE to one catalytic cysteine of MnmA although experimental evidence for the persulfide form of MnmA is lacking (6–8). MnmA, as the last element of the sulfur relay, introduces the sulfur atom into the tRNA substrate. Structural analysis of *E. coli* MnmA bound to tRNA in various states (initial tRNA binding, pre-reaction and adenylated intermediate) (Figure 1B) (8) strongly supported a key role for three neighbor-

*To whom correspondence should be addressed. Tel: +33 1 44 27 12 52; Fax: + 33 1 44 27 14 83; Email: beatrice.golinelli@college-de-france.fr
Correspondence may also be addressed to Frédéric Barras. Email: fbarras@pasteur.fr
†The authors wish it to be known that, in their opinion, the first two authors should be regarded as Joint First Authors.

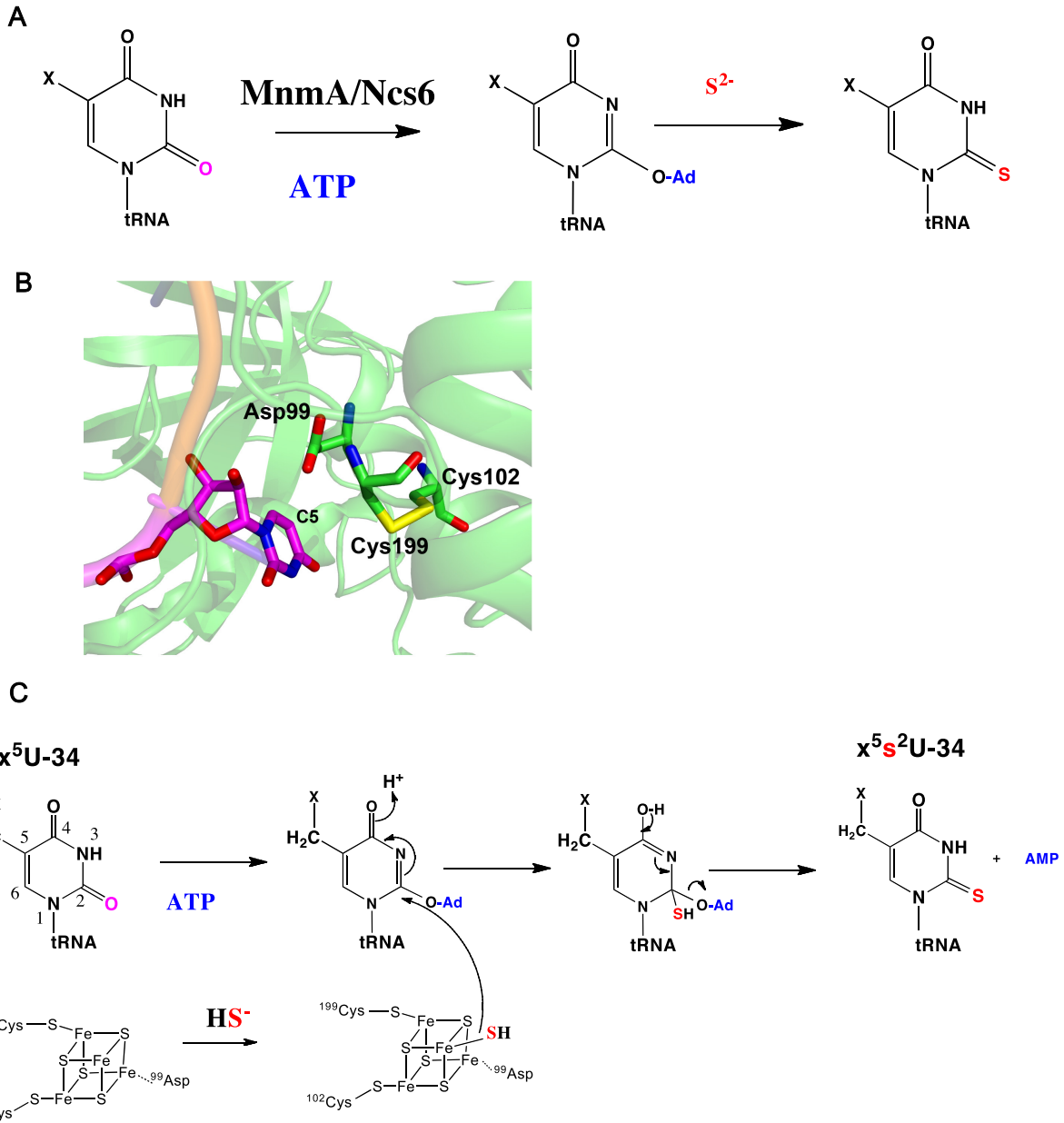

Figure 1. s^2U34-tRNA sulfuration and structure of *Escherichia coli* MnmA. (**A**) ATP-dependent reaction catalyzed by U34-tRNA thiolases through the formation of an adenylated intermediate. Ad stands for 'adenylate'. (**B**) Structure of the active site of tRNA-bound MnmA (PDB code: 2DET) with the catalytic residues (green) and the U34 target (magenta) in stick representation. Cys102 and Cys199 form a disulfide bond. The Asp99 O2 atom is located 4.5 Å away from the Cys199 SG atom. (**C**) New mechanism proposed for [4Fe–4S]-dependent U34 sulfuration by *E. coli* MnmA.

ing residues in U34-tRNA sulfuration: Asp99, Cys102 and Cys199 (making up the DXXC + C motif in the catalytic domain; Supplementary Figure S1). In the currently accepted mechanism, Cys199 is proposed to carry the active persulfide, Cys102, to assist sulfur transfer via formation of a disulfide bond with Cys199, whereas Asp99 could act as an acid/base catalyst to facilitate proton transfer (Supplementary Figure S2) (8).

IscS acts as a pleiotropic sulfur donor in the cell. In particular, it forms, together with a series of protein partners IscU, IscA, HscAB and Fdx, the well-conserved ISC [Fe–S] cluster biogenesis machinery, which builds and delivers [Fe–S] clusters to most, if not all, [Fe–S] cellular proteins (19–21). Early work established the role of IscS in s^2U34-tRNA modification in *E. coli* and *S. enterica* (6,16,22,23) but ruled out a role for the other ISC proteins in *S. enterica* (24), leading to the current belief that MnmA is not an [Fe–S] protein. This model was supported by the absence of such a cluster within the crystal structures of as-purified *E. coli* MnmA (8) and by the observation of a sulfuration activity by aerobically purified enzymes preparations under *in vitro* conditions, albeit very weak (6–8,25).

In contrast to the view presented above, we report here biochemical and spectroscopic results unambiguously

showing that *E. coli* MnmA can assemble a [4Fe–4S] cluster, most likely chelated by Asp99, Cys102 and Cys199, and that this cluster is absolutely needed for *in vitro* activity. Intriguingly, we found that *E. coli* cells retain s^2U34 biosynthesis in the Δ*iscUA* Δ*sufABCDSE* strain, lacking functional ISC and SUF [Fe–S] cluster assembly machineries, thus suggesting an original and yet undescribed way of maturation of MnmA.

MATERIALS AND METHODS

Media and growth conditions

Media used were Luria–Bertani (LB) rich medium or M9 minimal medium supplemented with glycerol (0.4%) and $MgSO_4$ (1 mM). L-Arabinose (Ara) (0.2%), casamino acids (0.05%), thiamine (50 μg ml^{-1}) and mevalonate (MV), 1 mM were added when required. Solid media contained 1.5% agar. Antibiotics were used at the following concentrations: chloramphenicol (Cam), 30 μg ml^{-1}; kanamycin (Kan), 30 μg ml^{-1}; spectinomycin (Spc), 100 μg ml^{-1}; and ampicillin (Amp), 100 μg ml^{-1}. Note that Kan was used at 80 μg ml^{-1} for transduction experiments involving the *ΔiscS* mutants as recipients. For growth at pH 7.0 or 4.5, cultures grown in LB rich medium were diluted 1:100 into 200 μl of LB or LB–HCl (pH 4.5) in 96-well plates. Growth was monitored using a TECAN spectrophotometer by recording OD_{600} every 10 min over 16 h at 37°C.

Strains and plasmids

All strains used in this study are *E. coli* K-12 MG1655 derivatives. The *mnmA* mutant, FBE584, was obtained by in-frame deletion of *mnmA* and replaced with a kanamycin cassette (26). FBE597 was obtained from the *E. coli* KEIO Knockout Collection (27) by P1 transducing the *mnmE::kan* allele into MG1655 background. The *mnmE::cam* mutant was constructed by deleting and replacing the *mnmE* gene with a chloramphenicol resistance encoding cassette giving rise to the FBE707 strain (26). The conditional RExBAD*mnmA* mutant, FBE583, was obtained by amplifying a fragment carrying the *aadA7I* (spectinomycin resistance gene) and *araC* genes by polymerase chain reaction (PCR) from TG1 spec RExBAD (FBE319) using the ML39 primers (28). The linear fragment was then inserted upstream of the *mnmA* gene in *E. coli* MG1655 carrying the λ red expression plasmid pKD46 (26). All mutants were P1-transduced into different *E. coli* K-12 backgrounds (Supplementary Table S1). The CF8310 strain, a MG1655 strain derivative carrying the T7 RNA polymerase encoding gene on a lambda prophage (DE3), was used as recipient for P1 transduction of Δ*mnmA::kan,* giving rise to the FBE598 strain. Strain FBE605 (Δ*iscUA* Δ*sufABCDSE* MVA^+, *kan*R p*iscR*::*lacZ Δlac*) is a MG1655 strain derivative, which can synthesize isopentenyl diphosphate from the introduced eukaryotic MVA-dependent pathway (29). Strain FBE605 was derived from BR404 (30) as follows. First, the CamR cassette was removed from the *suf* locus, yielding to BR412 that was used as a recipient for P1 transduction of the Δ*iscUA*::*cat* mutation, to generate FBE033. The Cat cassette was removed from the *iscUA* locus by using the pCP20 plasmid. PCR analysis was used to check the absence of the *iscUA* genes and the *suf* operon. DNA sequence analysis of the *isc* region was carried out and MVA-dependent viability was controlled. For all constructions, transductants were verified by PCR, using primers hybridizing upstream and downstream of the deleted gene. When necessary, antibiotic resistance cassettes were eliminated using plasmid pCP20 as described (31). Strains used in this study are listed in Supplementary Table S1.

Plasmid construction

To construct the pBAD*mnmA*$^+$ plasmid, the *mnmA* gene was first amplified from *E. coli* MG1655 chromosomal DNA using the ML40 primers, digested by EcoRI and XhoI and cloned into the EcoRI and SalI sites of pBAD24. The *mnmA* gene was also subcloned into the pET28a vector by PCR amplification from pBAD*mnmA*$^+$ to introduce the BamHI restriction site and the TEV nucleotide sequence in 5′ and the HindIII restriction site in 3′ using the ML52 primers. The PCR fragment was purified, digested by BamHI and HindIII and cloned into the BamHI and HindIII sites of pET28a. *mnmA* variants containing mutations were obtained by site-directed mutagenesis using the ML49–50-51 primers (NEB, E0554S). The sequence of the expression plasmids was confirmed by sequencing. Primers and plasmids used in this study are listed in Supplementary Tables S2 and S3, respectively.

Synthetic lethality test

Cells were cultivated in M9 minimal medium supplemented with 0.05% casamino acids and 0.4% glycerol overnight at 37°C. Saturated cultures were washed the next day twice with PBS and then diluted 1:50 into LB rich medium with or without 0.2% L-arabinose. Cultures were incubated at 37°C for 8 h. The optical density at 600 nm was measured over time.

Hydrogen peroxide sensitivity test

Overnight cultures were diluted using serial dilution in sterile PBS and 5 μl was directly spotted onto LB plates containing 1 mM H_2O_2. The plates were incubated overnight at 37°C before growth was recorded.

Overexpression of *E. coli* MnmA wild-type and the D99A-C102A and D99A-C102A-C199A variants

The *mnmA* gene was sub-cloned into the pET15b plasmid using a ligation independent cloning strategy by Eurofins to produce a 6His-MnmA protein construct whose 6His tag can be cleaved by the H3C protease. The $mnmA_{D99A\text{-}C102A}$ and $mnmA_{D99A\text{-}C102A\text{-}C199A}$ genes were sub-cloned into the pET28a plasmid. The plasmids were transformed into *E. coli* BL21(*DE3*) Star Codon Plus competent cells. One colony was used to inoculate 100–200 ml of LB medium supplemented with ampicillin or kanamycin (50 μg ml^{-1}) for MnmA wild-type and variants, respectively. 60 ml (20 ml) of this culture grown overnight at 37°C was used to inoculate 6 L (2 L) of LB medium supplemented with the

same antibiotic. Cultures were grown at 37°C to an OD_{600} 0.6–0.8, and overexpression was induced with 0.5 mM Isopropyl β-D-1-thiogalactopyranoside. After 4 h incubation at 37°C, cells were collected by centrifugation and stored at −20°C.

Purification of *E. coli* wild-type MnmA and variants

Cells were resuspended in 50 mM Tris-HCl (pH 7.5), 500 mM NaCl, 10% glycerol, containing RNase A (2 μg ml^{-1}), benzonase (1.6 U ml^{-1}, Sigma Aldrich), lysozyme (0.3 mg ml^{-1}), 1 mM PMSF PhenylMethylSulfonyl Fluoride, 1 mM β-mercaptoethanol and disrupted by sonication. Cells debris were removed by centrifugation at 25 000 rpm for 1 h at 4°C. The supernatant was then loaded on an immobilized metal affinity Ni-NTA column (HisTrap 5 ml, GE Healthcare) equilibrated in 50 mM Tris-HCl (pH 7.5), 200 mM NaCl, 1 mM PMSF and eluted with a linear gradient of 0–1 M imidazole. The proteins were collected, dialyzed twice against 1 L of 50 mM Tris-HCl (pH 7.5), 200 mM NaCl, 1 mM β-mercaptoethanol in the presence of the PreScission Protease (25 μg per mg wild-type MnmA) or TEV protease (43 μg/mg MnmA variants). Wild-type MnmA was further purified at 1 ml min^{-1} onto a gel filtration column (Hiload 26/60 Superdex 200, GE Healthcare) equilibrated with 50 mM Tris-HCl (pH 7.5), 200 mM NaCl, using an ÅKTA system. The as-purified proteins were concentrated to 24 mg ml^{-1} (wild-type) with an Amicon Ultra filter device (30 kDa cutoff, Millipore) or 4–5 $mg.ml^{-1}$ (variant) with an Amicon Ultra filter device (10 kDa cutoff, Millipore), frozen in liquid nitrogen and stored at −80°C.

The GST–3C-protease (PreScission, a gift from S. Mouilleron) was expressed using pGEX-2T recombinant plasmids. After induction at 25°C with 0.1 mM IPTG for 20 h, the protein was purified using glutathione–Sepharose chromatography.

[Fe–S] cluster reconstitution and purification of holo-MnmA wild-type and variants

The reconstitution of the [4Fe–4S] cluster and purification of holo-MnmA were performed in a glove box containing <0.5 ppm O_2. After incubation of 100 μM as-purified MnmA with 10 mM dithiothreitol for 10 min, a 5.5-fold molar excess of ferrous ammonium sulfate and L-cysteine, as well as 2 μM *E. coli* cysteine desulfurase CsdA, were added, and incubation was extended overnight at room temperature. After centrifugation for 20 min at 12 300 *g*, holo-MnmA was loaded onto a Superdex 200 increase 10/300 GL column (GE Sciences) equilibrated in 50 mM Tris-HCl (pH 7.5), 200 mM NaCl, 5 mM dithiothreitol (DTT). The peak containing the holo-MnmA was then concentrated to 10–19 mg/ml on a Vivaspin concentrator (10 kDa cutoff). The same protocol was used for analyzing the capacity of the variants to host [Fe–S] clusters.

Quantification methods

The Bradford method was used to quantify the protein (32). The Fish and Beinert methods were routinely used after cluster reconstitution to quantify iron and sulfide, respectively (33,34).

SEC-MALS

Size exclusion chromatography coupled with multi-angle light scattering (SEC-MALS) experiments were performed using an HPLC-MALS system (Shimadzu) equipped with light scattering detector (mini DAWN TREOS, Wyatt Technology), refractive index detector (Optilab T-rEX, Wyatt Technology) and UV detector (SPD-20A, Shimadzu). Holo-MnmA (100 μl at 2 mg ml^{-1}) was injected on a Superdex 200 10/300 GL increase column (GE Healthcare) equilibrated in 50 mM Tris-HCl (pH 7.5), 200 mM NaCl buffer, in the presence or absence of DTT at a flow rate of 0.5 $ml.min^{-1}$. Molar masses of proteins were calculated using the ASTRA 6.1 software (Wyatt Technology) using a refractive index increment (dn/dc) value of 0.183 ml g^{-1}.

CD analysis

Circular dichroism (CD) spectra were recorded on a Chirascan-plus CD Spectrometer (Applied Photophysics). The far ultraviolet spectra (195−260 nm) were measured at 20°C in quartz cells of 0.5 mm optical path length. The final concentration of MnmA proteins was 2 μM in 25 mM Tris-HCl (pH 7.5), 100 mM NaF. Spectra were acquired at a resolution of 1 nm, with time per points set at 1 s and a bandwidth of 1 nm. All spectra were corrected from the contribution of the buffer and are an average of ten accumulations.

Preparation of bulk tRNA and *in vitro* transcribed Ec-$tRNA^{Glu}$

Bulk tRNA from various *E. coli* strains was purified as reported (35). The *E. coli* $tRNA^{Glu}_{UUC}$ (Ec-$tRNA^{Glu}$) was synthesized *in vitro* by T7-RNA polymerase transcription as described in (36). Before use, the tRNA transcript was refolded by heating at 65°C for 15 min then 45°C for 15 min, and finally cooling at 4°C for 30 min.

In vitro enzyme assay

Holo-MnmA (1 or 10 μM) and Ec-$tRNA^{Glu}_{UUC}$ (15 μM) were incubated at 37°C in 100 μl of 50 mM Tris-HCl (pH 7.5), 200 mM NaCl in the presence of 0.25 mM ATP, 2.5 mM $MgCl_2$ and 1 mM Na_2S under anaerobic conditions for 60 min. The reaction was stopped by adding 1 μl of 3 M formic acid, followed by the addition of 3 μl of 1 M Tris (pH 8.5) to adjust the pH of the solution to 6.5.

tRNA digestion and analysis of modified nucleosides

tRNA (15 μM) was digested overnight in 100 μl of 50 mM Tris-HCl (pH 7.5), 200 mM NaCl, 0.1 mM $ZnSO_4$ at 37°C by nuclease P1 (two units, Sigma) followed by the addition of alkaline phosphatase for 2 h at 37°C (1 unit, Sigma). HPLC-tandem mass spectrometry analyses were performed with an ExionLC chromatographic system coupled with a QTRAP6500+ mass spectrometer (AB SCIEX INSTRUMENTS) equipped with a Turbo Spray IonDrive source used in the positive ionization mode. HPLC separation was carried out with a 2 × 150 mm, 2.7 μm Poroshell HPH-C18 column (Agilent, France) at

0.4 ml min^{-1} and at 35°C. A linear gradient of 0–15% acetonitrile in 0.1% formic acid over 7 min was used as the mobile phase. Mass spectrometry detection was carried out in the multiple reactions monitoring mode to obtain high sensitivity and specificity. The transitions used to quantify s^2U (or s^4U that has a similar fragmentation pattern) were 261→129 and 261→112, corresponding to the loss of ribose. Under the HPLC conditions used, s^2U is eluted faster (4.3 min) than s^4U (4.6 min). Quantification was performed by external calibration. The 5-methylaminomethyl-2-thiouridine (mnm^5s^2U) and 5-carboxymethylaminomethyl-2-thiouridine ($cmnm^5s^2U$) standards were synthesized via nucleophilic substitution of 5-pivaloyloxymethyl-2-thiouridine with methylamine or tetrabutylammonium salt of glycine, respectively, according to the previously described procedures (37). The structure and homogeneity of both nucleosides were confirmed by ^1H and ^{13}C NMR, mass spectrometry and reversed-phase HPLC analysis.

Characterization of the [4Fe–4S] cluster by UV-Visible and EPR spectroscopies

UV-visible absorption spectra were recorded in quartz cuvettes (1 cm optic path) under anaerobic conditions in a glove box on a Cary 100 UV-visible spectrophotometer equipped with optical fibers.

The EPR continuous wave measurements were performed on a spectrometer Bruker ELEXSYS-E500 operating at 9.38 GHZ, equipped with SHQE cavity cooled by a helium flow cryostat ESR 900 Oxford Instruments. The EPR spectra of frozen solution of 220 μM *E. coli* MmnA with reconstituted cluster, without treatment and reduced with 5.5 mM dithionite in 50 mM Tris-HCl (pH 7.5), 200 mM NaCl was recorded at 10, 15 and 20 K, under non-saturating conditions and using the following parameters: a microwave power of 2–10 mW, a modulation amplitude of 0.4 mT, a modulation frequency of 100 kHz and an accumulation of 4 scans. For the quantification of unpaired spins, a Cu-EDTA standard sample (200 μM) was used. The simulation of the EPR spectrum was performed with the Easyspin software (http://www.easyspin.org/).

RESULTS

Escherichia coli MnmA binds a [4Fe–4S] cluster

Escherichia coli MnmA with an N-terminal histidine tag was purified under aerobic conditions using Ni-affinity chromatography. The faint brownish color and the weak absorbance at 410 nm suggested the presence of an [Fe–S] cluster (Supplementary Figure S3A). The tag was then removed using the H3C protease and the protein was further purified by size-exclusion chromatography, which led to a mixture of monomeric and dimeric species, as shown by SEC-MALS analysis (Supplementary Figure S3B and S3C). Because the monomer/dimer ratio increases with DTT concentration (Supplementary Figure S3B), the dimer is formed by disulfide bonds between two monomers. As-purified MnmA retained a faint brownish color and its UV-visible spectrum exhibited a band at around 410 nm (Supplementary Figure S3D). These unexpected features, which disappeared upon further aerobic purification, strongly suggested the presence of an [Fe–S] cluster within the as-purified protein, which would be destroyed by air during purification, and prompted us to evaluate the potential of MnmA to assemble a well-defined cluster. For that purpose, *in vitro* reconstitution of the cluster was carried out by anaerobically treating the protein with ferrous iron and L-cysteine in the presence of a cysteine desulfurase, as a source of sulfur. The protein was then purified by size-exclusion chromatography, also under anaerobic conditions, leading to a homogeneous brownish protein, indicative of the presence of an [Fe–S] cluster in the protein that was subsequently called holo-MnmA. SEC-MALS analysis (Supplementary Figure S3E) indicated that holo-MnmA is almost exclusively in the monomeric form in solution, the molar mass of the protein being 40.0 ± 2.6 kDa, close to the theoretical molar mass of the monomer (41 kDa).

Quantification of the protein-bound iron and sulfur content gave 3.02 ± 0.2 Fe and 3.9 ± 0.3 S per MnmA monomer, consistent with the presence of one [4Fe–4S] cluster per monomer. Accordingly, the UV-visible spectrum of purified holo-MnmA displays a broad absorption band at around 410 nm that is specifically characteristic for the presence of a [4Fe–4S] cluster (Figure 2A). Anaerobic addition of dithionite to holo-MnmA led to a rapid decrease in the intensity of the 410 nm absorption band, suggesting a fast reduction of the cluster (Figure 2A). The frozen solutions of holo-MnmA, before and after reduction, were analyzed by continuous wave EPR spectroscopy at different temperatures (Figure 2B and Supplementary Figure S3F). No EPR signal was observed for holo-MnmA solution, suggesting an $S = 0$ $[4Fe–4S]^{2+}$ state, and excluding $S = 1/2$ paramagnetic clusters such as $[4Fe–4S]^{+}$ or $[3Fe-4S]^{+}$. Upon reduction, the EPR spectrum of the protein recorded at 15 K exhibited a signal with a rhombic g tensor ($g_x = 1.88$, $g_y = 1.92$, $g_z = 2.045$) characteristic of the $S = 1/2$ $[4Fe–4S]^{+}$ state (Figure 2B). Temperature variations allowed to discriminate between a $[2Fe-2S]^{+}$ cluster and a $[4Fe–4S]^{+}$ cluster because of their different spin relaxation behaviors (38). At 40 K, the EPR lines of the reduced holo-MnmA sample broadened beyond recognition (Supplementary Figure S3F), in agreement with the presence of a $[4Fe–4S]^{+}$ cluster, which usually cannot be detected above 35 K, in contrast to $[2Fe–2S]^{+}$ clusters. Quantification with Cu-EDTA standard solution indicated the presence of around 0.5 spin per holo-MnmA monomer.

The [4Fe–4S] cluster is required for the tRNA sulfuration activity of *E. coli* MnmA

The sulfuration activity of *E. coli* MnmA was tested using *in vitro* transcribed Ec-$tRNA^{Glu}$ as a substrate in the presence of ATP, Mg^{2+} and inorganic sulfide, a sulfur donor often used in enzyme sulfuration assays (39–41). The thiolated nucleosides were quantified after digestion of the tRNA products by nuclease P1 and alkaline phosphatase. The s^2U product was first identified by its elution position after HPLC-coupled mass spectrometry (MS), then quantified by MS/MS using a synthetic s^2U standard (Figure 2C). The fragment spectrum corresponding to the loss of sugar (-132) was monitored (Figure 2D). Holo-MnmA (1

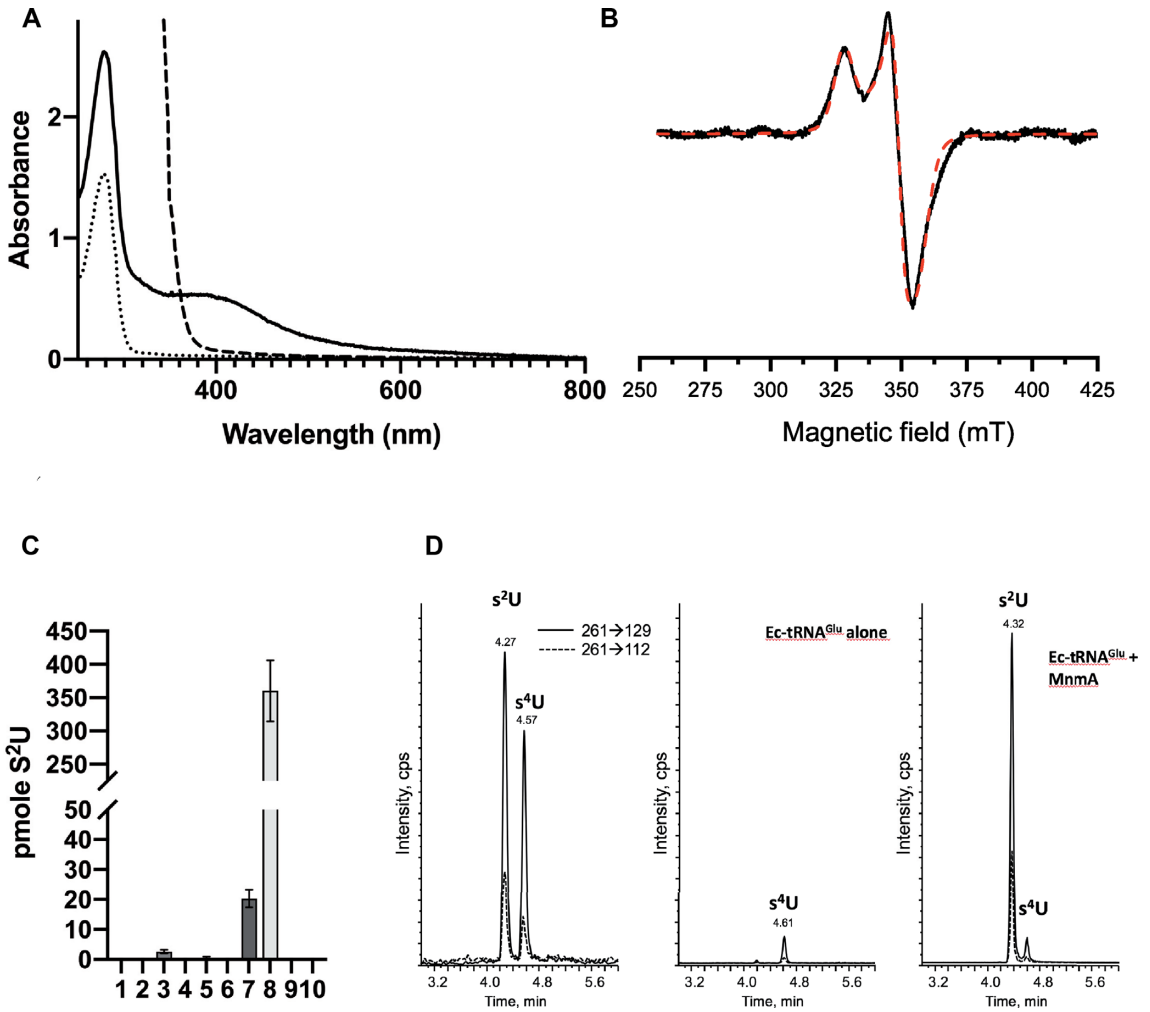

Figure 2. Spectroscopic and enzymatic characterizations of *E. coli* MnmA. (**A**) UV-visible spectra of 40 μM apo-MnmA (dotted line), 40 μM holo-MnmA (thick line) and reduced holo-MnmA after 20 min of incubation with 1 mM dithionite (dashed line). The spectra were recorded with 40 μM protein in 50 mM Tris-HCl (pH 7.5), 200 mM NaCl, 5 mM DTT in 1 cm (apo-MnmA and reduced holo-MnmA) or 1 mm (holo-MnmA) pathlength cuvettes and normalized. (**B**) X-band EPR spectrum (10 mW microwave power; modulation amplitude of 0.4 mT) of 220 μM holo-MnmA reduced with 5.5 mM dithionite at 15 K. The experimental (black solid line) and simulated (dashed line) spectra are superimposed. The cluster was simulated with the following values of the g-tensor: $g_x = 1.880$, $g_y = 1.920$, $g_z = 2.045$ and Gaussian distribution deviations $\sigma(g_x) = 0.04$, $\sigma(g_y) = 0.02$, $\sigma(g_z) = 0.04$. (**C**) *In vitro* tRNA sulfuration activity tests of MnmA under anaerobic conditions. After tRNA digestion, s^2U was separated by HPLC-MS/MS and quantified using a synthetic s^2U standard. The data shown are mean values based on three different experiments, with the standard error of the mean indicated as a bar. *In vitro* transcribed Ec-tRNA^{Glu} (15 μM) was incubated for 1 h at 37°C in 50 mM Tris (pH 7.5), 200 mM NaCl with apo or holo-MnmA (wild-type or mutant) in the presence or absence of 1 mM Na_2S, 2.5 mM $MgCl_2$, 0.25 mM ATP. Ec-tRNA^{Glu} alone 15 μM (**1**), apo-MnmA 1 μM (**2**) or 10 μM (**3**), 1 μM holo-MnmA and no Na_2S (**4**), no $MgCl_2$ (**5**) or no ATP (**6**), holo-MnmA 1 μM (**7**) or 10 μM (**8**), 1 μM holo-MnmA$_{D99A-C102A}$ mutant (**9**) or 1 μM holo-MnmA$_{D99A-C102A-C199A}$ mutant (**10**). (**D**) HPLC MS/MS detection of s^2U and s^4U (m/z 261). Samples were analyzed using the two transitions 261→129 and 261→112; the most intense one corresponds to the loss of the ribose moiety. Left: mixture of s^2U and s^4U synthetic standards (0.5 pmole injected); middle: Ec-tRNA^{Glu} alone after hydrolysis; right: Ec-tRNA^{Glu} (15 μM) after incubation with holo-MnmA (10 μM) in the presence of Na_2S, ATP, $MgCl_2$ and hydrolysis.

μM) was able to catalyze sulfuration of tRNA (15 μM) in contrast to apo-MnmA (1 or 10 μM) (Figure 2C). Moreover, the sulfur atom that was inserted into the nucleoside is derived exclusively from the inorganic sulfide salt, and not from the [4Fe–4S] cluster, since no sulfuration could be observed in the absence of sulfide. These control experiments indicated that the cluster and inorganic sulfide were required for the tRNA sulfuration activity of MnmA. Moreover, the amount of product formed increased with enzyme concentration (1 μM versus 10 μM in Figure 2C). Mg-ATP was also required, in agreement with its role in activating the substrate via adenylation of the C2 oxygen atom (Figure 1A and Supplementary Figure S2) (8).

MnmA is necessary for *E. coli* to resist to stress

It was previously shown that *mnmA* mutation in *E. coli* leads to reduced growth rate (14). We reproduced this observation (Figure 3A) and also noticed that the mutant exhibited a small colony phenotype when plated on rich medium (Figure 3C). We constructed the Δ*mnmA* strain and checked by HPLC-MS that the bulk tRNA from this strain did not contain mnm^5s^2U nor $cmnm^5s^2U$ (Table 1). By monitoring growth in liquid culture, we found that the Δ*mnmA* strain showed slower growth in the presence of a mild acid stress (i.e. growth medium at pH 4.5) (Figure 3B) and that it exhibited hypersensitivity to H_2O_2 (Figure 3C). Note that sur-

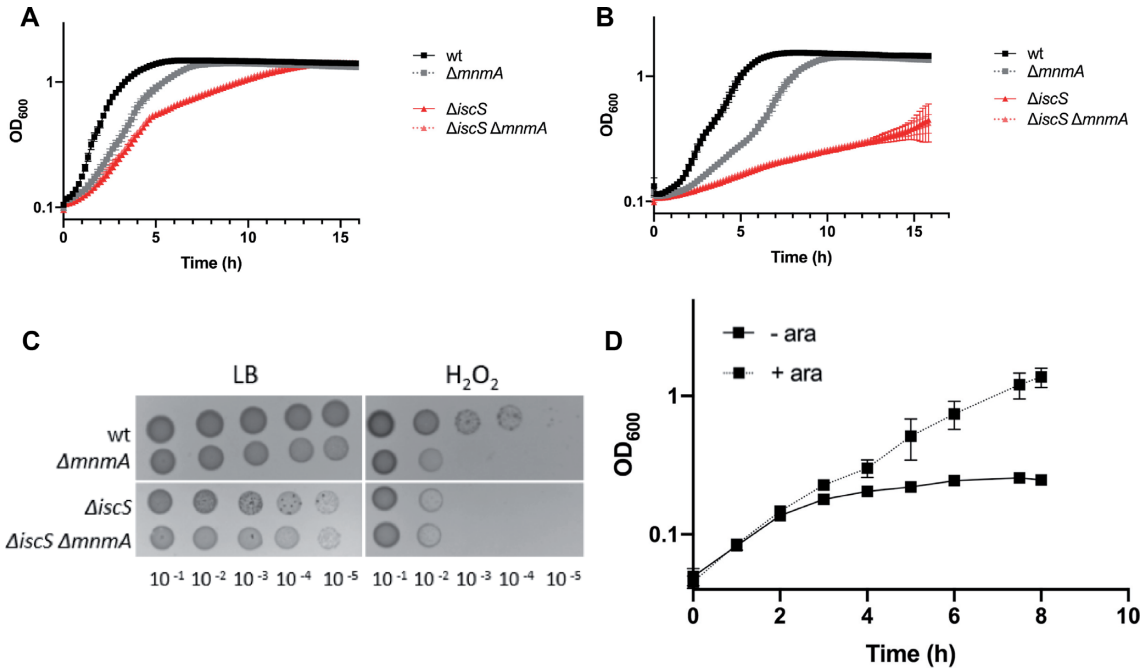

Figure 3. Phenotypes of Δ*mnmA* and derivative strains. (**A**) Growth in LB pH 7.0 medium. Strains studied are wild-type (wt) (FBE051), *ΔmnmA* (FBE584), *ΔiscS* (FBE653) and *ΔiscS ΔmnmA* (FBE703). Data are representative of three independent experiments (n = 3). (**B**) Growth in LB–HCl (pH 4.5). Strains studied are wild-type (wt) (FBE051), *ΔmnmA* (FBE584), *ΔiscS* (FBE653) and *ΔiscS ΔmnmA* (FBE703), (n=3). (**C**) Hypersensitivity of *ΔmnmA* to H_2O_2 (1 mM). Strains tested are wt, *ΔmnmA*, *ΔiscS* and *ΔiscS ΔmnmA*. Each spot represents a 10-fold serial dilution (*n* = 3). (**D**) The *ΔmnmE* and *ΔmnmA* mutations are lethal synthetic in *E. coli*. The RExBADmnmA *ΔmnmE* strain (FBE601) was grown in LB rich medium without (- ara) or with (+ ara) 0.2% L-arabinose, (*n* = 3).

Table 1. Analysis of s^2C, mnm^5s^2U and $cmnm^5s^2U$ content (in pmoles) of bulk tRNA (15 μM) from various strains (mean of three measurements)

	s^2C	$cmnm^5s^2U$	mnm^5s^2U
Wild-type	9.5 ± 1.7	107.6 ± 39.8	1080.7 ± 647.0
Δ*mnmA*	14.8 ± 2.2	0.0 ± 0.1	1.9 ± 1.0
Δ*iscUA Δsuf*ABCDSE	0.0 ± 0.0	64.5 ± 20.9	1421.9 ± 601.7
Δ*ttcA*	0.4 ± 0.1	68.0 ± 44.4	1756.1 ± 1003.5

vival plate assays run in parallel showed that the viability of the *mnmA* strain was not impaired at pH 4.5.

U34-tRNA modification pathway in *E. coli*

Biochemical studies together with a genetic approach coupled with mass spectrometry (ribonucleome analysis) have shown that MnmA receives sulfur from the IscS cysteine desulfurase (6,22) and the TusABCDE sulfur relay pathway (7). Thus, the prediction is that the *ΔiscS* strain should exhibit defects similar to those of the Δ*mnmA* strain, as shown in *S. enterica* (16). The *ΔiscS* mutation was found to cause extreme sensitivity to pH 4.5, even to a larger extent than that caused by the Δ*mnmA* mutation (Figure 3B). Such a feature has never been described for IscS so far. Introducing the Δ*mnmA* mutation in a *ΔiscS* background did not worsen the defect (Figure 3B), in line with the idea that MnmA depends upon IscS for getting sulfur. Similarly, when challenging the strains with H_2O_2 (Figure 3C), the *ΔiscS* strain displayed hypersensitivity comparable to that of the Δ*mnmA* strain, and the combination of both deletions failed to enhance the defect.

Besides hypersensitivity to H_2O_2, we wished to set-up another MnmA-associated phenotypic test. For this, we took advantage of the synthetic lethality between *mnmA* and *mnmE* mutations. MnmE, along with MnmG, adds the aminomethyl and carboxymethylaminomethyl groups to the C5 position of U34 (42). We constructed a strain named RExBAD*mnmA,* in which expression of the *mnmA* gene was under the control of an arabinose inducible promoter and tested whether it could accommodate a Δ*mnmE* mutation. We observed that the Δ*mnmE* mutation could be introduced by transduction only when arabinose was added to the medium (Figure 3D). This confirmed that a strain lacking both *mnmA* and *mnmE* is not viable, as previously shown by using a strain, in which the *mnmA* gene was deleted and the *mnmE* gene put under the control of an arabinose inducible promoter (42).

Then, we reasoned that if *iscS* was required for MnmA to function, then a strain carrying both *ΔiscS* and *ΔmnmE* should not be viable. Therefore, we asked whether we could introduce a *ΔiscS* mutation into a Δ*mnmE* mutant. The result was negative, suggesting that a *ΔiscS* mutation recapitulated the Δ*mnmA* mutation, in agreement with IscS providing the sulfur atom to MnmA.

Taken together, these genetic analyses showed that the *mnmA* gene is crucial for *E. coli* to grow under both balanced and stress conditions, and established its close functional interaction with *iscS*, in agreement with early studies in *S. enterica* (23).

The ligands of the [4Fe–4S] cluster are most likely Asp99, Cys102 and Cys199

The D99A, C102S and C199A mutants of *E. coli* MnmA were reported to lack *in vitro* U34-tRNA sulfuration activity using cysteine as the sulfur donor, and the IscS and Tus proteins as sulfur carriers (8). We produced the double D99A-C102A and the triple D99A-C102A-C199A mutants (Supplementary Figure S4). Both mutants were correctly folded, as shown by their circular dichroism spectrum, which did not differ from that of the wild-type protein (Supplementary Figure S4F). After cluster reconstitution, they both almost completely lost the absorption band at 410 nm (Supplementary Figure S4G) and were shown to contain very little Fe, namely 0.46 ± 0.03 and 0.25 ± 0.05 iron per MnmA monomer, respectively. Finally, they did not exhibit any catalytic activity (Figure 2C, columns 9 and 10) in standard *in vitro* assays with sulfide used as a sulfur donor. Therefore, the mutagenesis results point out Asp99, Cys102 and Cys109 as being involved in cluster binding and catalysis (Figure 1B) (8). But one cannot unambiguously conclude on the *in vitro* analysis of only the double and triple mutant variants that all three residues contribute to ligation. Yet, we did not analyze the single variants because, in many instances, a single mutation of a cluster ligand was shown to be not sufficient to disrupt cluster ligation (43,44). Therefore, in addition, we tested the functional importance of the Asp99, Cys102 and Cys109 residues by changing each of them to alanine and testing the activity of the resulting single mutants *in vivo* using the series of phenotypic tests described above (Supplementary Figure S5). When expressed *in trans* from plasmids, all mutated variants, namely D99A, C102A and C109A failed to (i) suppress growth rate defects of the Δ*mnmA* recipient in rich medium (Supplementary Figure S5A, top), (ii) suppress hypersensitivity of the Δ*mnmA* strain to acid (Supplementary Figure S5A, bottom) and oxidative stress (Supplementary Figure S5B) and (iii) allow growth in the absence of arabinose in the RExBAD*mnmA* Δ*mnmE* containing background (Supplementary Figure S5C). Note that expression of all three alleles gave rise to large amounts of soluble protein so that the possibility of a destabilizing effect of the introduced mutations was ruled out (Supplementary Figure S5D). Hence, based upon their inability to complement different defects of the Δ*mnmA* mutant, we concluded that substitution of Asp99, Cys102 or Cys109 by alanine yielded a nonfunctional MnmA protein. Altogether, the simplest interpretation of the *in vitro* characterization of the mutants and the *in vivo* complementation assays is that Asp99, Cys102 and Cys109 are the ligands of the [4Fe–4S] cluster.

Biosynthesis of mnm^5s^2U and $cmnm^5s^2U$ in tRNAs occurs in the absence of the ISC and SUF [Fe–S] cluster biogenesis systems

Since maturation of [Fe–S] proteins in *E. coli* relies on the two ISC and SUF machineries, we analyzed the s^2U content in bulk tRNA from the *ΔiscUA ΔsufABCDSE* strain (29) after tRNA digestion and HPLC-MS analysis (Table 1) to check whether MnmA maturation also uses these pathways. The *ΔiscUA ΔsufABCDSE* strain is not viable but can be grown by introducing the eukaryotic [Fe–S]-independent mevalonate-dependent isoprenoid biosynthesis pathway (29) to supply isopentenyl diphosphate, which is essential and normally synthesized by the [Fe–S] dependent IspG/IspH proteins. First, we observed that s^2C was absent in bulk tRNA from the mutated strain (Table 1), in full agreement with TtcA, the unique enzyme responsible for s^2C formation, requiring a [4Fe–4S] cluster (39) assembled by the ISC system (24). Then, we compared the content in mnm^5s^2U and $cmnm^5s^2U$ in bulk tRNA from a wild-type and the *ΔiscUA ΔsufABCDSE* strains. Unexpectedly, we found that the amounts of mnm^5s^2U and $cmnm^5s^2U$ from bulk tRNA in the mutant strain were comparable to those in the wild-type strain. This suggests that [Fe–S] cluster biogenesis of the *E. coli* MnmA protein can occur in the absence of the ISC and SUF systems.

DISCUSSION

We show here that MnmA, the only *E. coli* enzyme responsible for the sulfuration of U34 at C2 position in tRNAs (Figure 1A), assembles a [Fe–S] cluster. Moreover, the presence of this cluster proved essential for activity, under standard sulfuration assays previously used for other tRNA-sulfurating [Fe–S] enzymes such as TtcA (39) and TtuA (41). As a further confirmation of the functionality of the cluster, no *in vitro* activity could be obtained using MmnA variants, in which the residues that presumably bind the cluster (Asp99, Cys102 and Cys199) were changed into alanine. The occurrence of a [4Fe–4S] cluster was clearly established by Fe and S quantification and from UV-visible and EPR spectroscopic characteristic features, after cluster reconstitution under anaerobic conditions. Interestingly, residual cluster was also unambiguously observed within the as-purified protein before any chemical treatment, indicating that MnmA carried a cluster within the cell as well.

Shigi *et al.* recently reported that MnmA from *Thermus thermophilus* also contains an active [4Fe–4S] cluster (43). However, the authors proposed that MnmA proteins should be subdivided into [Fe–S]-containing and [Fe–S]-independent types (43). In the first C-type class, the three cysteines from the CXXC + C motif would ligate the cluster, such as in the *T. thermophilus* enzyme. The second D-type class would harbor a DXXC + C motif instead, like in the E. coli enzyme, which would be unable to bind a cluster. However, our results are strongly in agreement with Asp99, Cys102 and Cys199 of the DXXC + C motif being the ligands of the cluster of *E. coli* MnmA. Indeed, both the D99A-C102A and D99A-C102A-C199A mutants were unable to assemble a [4Fe–4S] cluster *in vitro*, in agreement with the observation that the D99A, C102A and C199A mutants were not able to rescue the growth phenotype of the Δ*mnmA* strain *in vivo*. It is interesting to note that Asp99, Cys102 and Cys199 are in close proximity to each other in the crystal structure of apo-MnmA (8), the only 3D structure available so far, and with the appropriate configuration for binding a [Fe–S] cluster (Figure 1B). In fact, amino acids other than cysteine can act as [Fe–S] ligands, such as histidine, glutamate, arginine and threonine (45). There are also precedents for aspartate as a ligand of a [4Fe–4S] or a [2Fe-2S] cluster, such as in ferrodoxin from hyperthermophilic

archaea (46,47), in a nitrogenase-like enzyme named protochlorophyllide reductase (48,49), in a transcriptional regulator (50) and in IscA, involved in [Fe–S] cluster assembly (51).

Given that Ncs6-type proteins also use a cluster for s^2U34 formation in tRNAs (52) (PDB code: 6SCY), the biochemical findings presented here lead us to propose that this sulfuration reaction depends on a [4Fe–4S] enzyme in all organisms and in mitochondria (9) (Supplementary Figure S1). More specifically, we propose that C-type and D-type MnmA are all [Fe–S] enzymes.

In Figure 1C, we propose a tentative mechanism for the holo-MnmA form, in which the cluster, adjacent to the substrate, serves to bind and activate a hydrosulfide nucleophilic substrate for subsequent attack on C2 from U34 to displace the AMP leaving group and form the final C–S bond in the product. A cluster with only three protein-bound ligands is appropriate for such a function since it provides a free coordination site on the fourth Fe atom where hydrosulfide can bind (53). We and others previously proposed a similar mechanism with the involvement of a [4Fe-5S] intermediate for TtuA, another thiouridine synthetase that targets position 54 in tRNA (41,54,55), and for TtcA responsible for the formation of s^2C32-tRNA (39). While more studies are required to firmly establish such a mechanism for tRNA thiolation enzymes, we have recently structurally characterized a relevant [4Fe-5S] catalytic intermediate during the desulfuration of 4-thiouracil by thiouracil desulfidase TudS (56), which thus provides a unique precedent for this class of intermediate clusters. Obviously, this mechanism excludes persulfides as key reaction intermediates, as proposed previously, since the cysteines of the active site proposed to carry the persulfide function are engaged as ligands of the [4Fe–4S] cluster.

As a consequence of the results reported here, we need to examine why an [Fe–S] cluster in *E. coli* MnmA was previously excluded, especially considering its essential catalytic role. First, the conclusion that MnmA could not be an [Fe–S] enzyme came from an early study examining the s^4U and mnm^5s^2U levels in ISC defective backgrounds; i.e. the *ΔiscU*, *ΔhscA*, *Δfdx* and *ΔiscA* strains showed wild-type like levels, while both s^2C and ms^2io^6A levels were found altered (24). It was concluded that downstream IscS, which is the shared sulfur source for the four reactions, two distinct routes were likely to occur for biosynthesis of thiolated nucleotides in tRNA: the [Fe–S]-dependent route, responsible for the formation of s^2C and ms^2io^6A, and the [Fe–S]-independent route, leading to s^4U and mnm^5s^2U. Therefore, previous MnmA preparations, purified exclusively under aerobic conditions, have not been analyzed for the presence of small amounts of protein-bound clusters (6–8), as we did here. It is well known that most clusters, and more specifically those with a labile coordination site, like in aconitase (57) or radical-SAM enzymes (58), are very sensitive to air and degrade during purification, generally leading to colorless protein solutions. Second, while these seemingly 'cluster-free' enzyme preparations were active, the reported activities were very weak, despite very large, far from catalytic, amounts of protein used (MnmA:tRNA ratios of 1:1 (6), 2.1:1 (7), 4:1 (8) or 6.4:1 (25). It is tempting to suggest that any measured activity might have been due to the presence of a small fraction of holo form in the as-purified MnmA, as we observed it here.

To date, maturation of all tested [Fe–S] proteins in *E. coli* has been found to depend upon ISC, SUF or both systems. Therefore, after having shown that MnmA contains an [Fe–S] cluster, we reinvestigated the contribution of ISC and/or SUF to mature MnmA. Surprisingly, the mnm^5s^2U/$cmnm^5s^2U$ content in tRNAs of the *ΔiscUA ΔsufABCDSE* strain was comparable to that in wild-type cells, arguing against the involvement of either machinery for maturation of MnmA. This result is consistent with previous work by Björk's (24) and Leimkühler's groups (59), who showed that ISC and SUF were dispensable for s^2U34 biosynthesis. Thus, to explain the s^2U content of tRNAs in the mutated strain, we are forced to entertain the possibility for MnmA to be targeted by an as yet unknown [Fe–S] cluster biogenesis pathway, which our current studies are aiming to identify.

DATA AVAILABILITY

All data are available in the manuscript; strains and constructs are available on request.

SUPPLEMENTARY DATA

Supplementary Data are available at NAR Online.

ACKNOWLEDGEMENTS

We thank the French EPR CNRS Facility, Infrastructure de Recherche Renard (IR 3443); the Macromolecular Interaction Platform of I2BC for use of its facilities and expertise; Ludovic Pecqueur for maintenance of the glove boxes; Bruno Faivre for advice in the purification experiments; Djemel Hamdane for assistance in CD experiments, Simon Arragain and Ornella Bimai for fruitful discussions that initiated this project; and the SAMe Unit members for discussion, technical help and suggestions.

FUNDING

Centre National de la recherche Scientifique and French State Program 'Investissements d'Avenir' [LABEX DYNAMO, ANR-11-LABX-0011, IBEID ANR-10-LABX-62]; Institut Pasteur. Funding for open access charge: LABEX DYNAMO.
Conflict of interest statement. None declared.

REFERENCES

1. El Yacoubi,B., Bailly,M. and de Crecy-Lagard,V. (2012) Biosynthesis and function of posttranscriptional modifications of transfer RNAs. *Annu. Rev. Genet.*, **46**, 69–95.
2. Boccaletto,P., Machnicka,M.A., Purta,E., Piatkowski,P., Baginski,B., Wirecki,T.K., de Crecy-Lagard,V., Ross,R., Limbach,P.A., Kotter,A. *et al.* (2018) MODOMICS: a database of RNA modification pathways. 2017 update. *Nucleic Acids Res.*, **46**, D303–D307.
3. Agris,P.F., Narendran,A., Sarachan,K., Vare,V.Y.P. and Eruysal,E. (2017) The importance of being modified: the role of RNA modifications in translational fidelity. *Enzymes*, **41**, 1–50.
4. Ranjan,N. and Rodnina,M.V. (2016) tRNA wobble modifications and protein homeostasis. *Translation (Austin)*, **4**, e1143076.

5. Schaffrath,R. and Leidel,S.A. (2017) Wobble uridine modifications—a reason to live, a reason to die?! *RNA Biol.*, **14**, 1209–1222.
6. Kambampati,R. and Lauhon,C.T. (2003) MnmA and IscS are required for in vitro 2-thiouridine biosynthesis in *Escherichia coli*. *Biochemistry*, **42**, 1109–1117.
7. Ikeuchi,Y., Shigi,N., Kato,J., Nishimura,A. and Suzuki,T. (2006) Mechanistic insights into sulfur relay by multiple sulfur mediators involved in thiouridine biosynthesis at tRNA wobble positions. *Mol. Cell*, **21**, 97–108.
8. Numata,T., Ikeuchi,Y., Fukai,S., Suzuki,T. and Nureki,O. (2006) Snapshots of tRNA sulphuration via an adenylated intermediate. *Nature*, **442**, 419–424.
9. Umeda,N., Suzuki,T., Yukawa,M., Ohya,Y., Shindo,H., Watanabe,K. and Suzuki,T. (2005) Mitochondria-specific RNA-modifying enzymes responsible for the biosynthesis of the wobble base in mitochondrial tRNAs. Implications for the molecular pathogenesis of human mitochondrial diseases. *J. Biol. Chem.*, **280**, 1613–1624.
10. Dewez,M., Bauer,F., Dieu,M., Raes,M., Vandenhaute,J. and Hermand,D. (2008) The conserved Wobble uridine tRNA thiolase Ctu1–Ctu2 is required to maintain genome integrity. *Proc. Natl. Acad. Sci. USA*, **105**, 5459–5464.
11. Noma,A., Sakaguchi,Y. and Suzuki,T. (2009) Mechanistic characterization of the sulfur-relay system for eukaryotic 2-thiouridine biogenesis at tRNA wobble positions. *Nucleic Acids Res.*, **37**, 1335–1352.
12. Nakai,Y., Nakai,M. and Hayashi,H. (2008) Thio-modification of yeast cytosolic tRNA requires a ubiquitin-related system that resembles bacterial sulfur transfer systems. *J. Biol. Chem.*, **283**, 27469–27476.
13. Grosjean,H., Breton,M., Sirand-Pugnet,P., Tardy,F., Thiaucourt,F., Citti,C., Barre,A., Yoshizawa,S., Fourmy,D., de Crecy-Lagard,V. *et al.* (2014) Predicting the minimal translation apparatus: lessons from the reductive evolution of mollicutes. *PLos Genet.*, **10**, e1004363.
14. Armengod,M.E., Meseguer,S., Villarroya,M., Prado,S., Moukadiri,I., Ruiz-Partida,R., Garzón,M.J., Navarro-González,C. and Martínez-Zamora,A. (2014) Modification of the wobble uridine in bacterial and mitochondrial tRNAs reading NNA/NNG triplets of 2-codon boxes. *RNA Biol.*, **12**, 1495–1507.
15. Nilsson,K., Jager,G. and Björk,G.R. (2017) An unmodified wobble uridine in tRNAs specific for glutamine, lysine, and glutamic acid from *Salmonella enterica serovar typhimurium* results in nonviability-due to increased missense errors? *PLoS One*, **12**, e0175092.
16. Nilsson,K., Lundgren,H.K., Hagervall,T.G. and Bjork,G.R. (2002) The cysteine desulfurase IscS is required for synthesis of all five thiolated nucleosides present in tRNA from *Salmonella enterica serovar typhimurium*. *J. Bacteriol.*, **184**, 6830–6835.
17. Kobayashi,K., Ehrlich,S.D., Albertini,A., Amati,G., Andersen,K.K., Arnaud,M., Asai,K., Ashikaga,S., Aymerich,S., Bessieres,P. *et al.* (2003) Essential *Bacillus subtilis* genes. *Proc. Natl. Acad. Sci. USA*, **100**, 4678–4683.
18. Kotera,M., Bayashi,T., Hattori,M., Tokimatsu,T., Goto,S., Mihara,H. and Kanehisa,M. (2010) Comprehensive genomic analysis of sulfur-relay pathway genes. *Genome Inform*, **24**, 104–115.
19. Fontecave,M., Py,B., Ollagnier de Choudens,S. and Barras,F. (2008) From iron and cysteine to iron-sulfur clusters: the biogenesis protein machineries. *EcoSal Plus*, **3**, doi:10.1128/ecosalplus.3.6.3.14.
20. Roche,B., Aussel,L., Ezraty,B., Mandin,P., Py,B. and Barras,F. (2013) Iron/sulfur proteins biogenesis in prokaryotes: formation, regulation and diversity. *Biochim. Biophys. Acta*, **1827**, 455–469.
21. Blanc,B., Gerez,C. and Ollagnier de Choudens,S. (2015) Assembly of Fe/S proteins in bacterial systems: biochemistry of the bacterial ISC system. *Biochim. Biophys. Acta*, **1853**, 1436–1447.
22. Lauhon,C.T. (2002) Requirement for IscS in biosynthesis of all thionucleosides in *Escherichia coli*. *J. Bacteriol.*, **184**, 6820–6829.
23. Lundgren,H.K. and Björk,G.R. (2006) Structural alterations of the cysteine desulfurase IscS of *Salmonella enterica serovar typhimurium* reveal substrate specificity of IscS in tRNA thiolation. *J. Bacteriol.*, **188**, 3052–3062.
24. Leipuviene,R., Qian,Q. and Björk,G.R. (2004) Formation of thiolated nucleosides present in tRNA from *Salmonella enterica* serovar *typhimurium* occurs in two principally distinct pathways. *J. Bacteriol.*, **186**, 758–766.
25. Black,K.A. and Dos Santos,P.C. (2015) Abbreviated pathway for biosynthesis of 2-thiouridine in *Bacillus subtilis*. *J. Bacteriol.*, **197**, 1952–1962.
26. Datsenko,K.A. and Wanner,B.L. (2000) One-step inactivation of chromosomal genes in *Escherichia coli* K-12 using PCR products. *Proc. Natl. Acad. Sci. USA*, **97**, 6640–6645.
27. Baba,T., Ara,T., Hasegawa,M., Takai,Y., Okumura,Y., Baba,M., Datsenko,K.A., Tomita,M., Wanner,B.L. and Mori,H. (2006) Construction of *Escherichia coli* K-12 in-frame, single-gene knockout mutants: the Keio collection. *Mol. Syst. Biol.*, **2**, 2006.0008.
28. Roux,A., Beloin,C. and Ghigo,J.M. (2005) Combined inactivation and expression strategy to study gene function under physiological conditions: application to identification of new *Escherichia coli* adhesins. *J. Bacteriol.*, **187**, 1001–1013.
29. Loiseau,L., Gerez,C., Bekker,M., Ollagnier-de-Choudens,S., Py,B., Sanakis,Y., Teixeira-de-Mattos,J., Fontecave,M. and Barras,F. (2007) ErpA, an iron–sulfur (Fe–S) protein of the A-type essential for respiratory metabolism in *Escherichia coli*. *Proc. Natl. Acd. Sci. USA*, **104**, 13626–13631.
30. Roche,B., Huguenot,A., Barras,F. and Py,B. (2015) The iron-binding CyaY and IscX proteins assist the ISC-catalyzed Fe-S biogenesis in *Escherichia coli*. *Mol. Microbiol.*, **95**, 605–623.
31. Cherepanov,P.P. and Wackernagel,W. (1995) Gene disruption in *Escherichia coli*: TcR and KmR cassettes with the option of Flp-catalyzed excision of the antibiotic-resistance determinant. *Gene*, **158**, 9–14.
32. Bradford,M.M. (1976) A rapid and sensitive method for the quantitation of microgram quantities of protein utilizing the principle of protein-dye binding. *Anal. Biochem.*, **72**, 248–254.
33. Beinert,H. (1983) Semi-micro methods for analysis of labile sulfide and of labile sulfide plus sulfane sulfur in unusually stable iron-sulfur proteins. *Anal. Biochem.*, **131**, 373–378.
34. Fish,W.W. (1988) Rapid colorimetric micromethod for the quantitation of complexed iron in biological samples. *Methods Enzymol.*, **158**, 357–364.
35. Buck,M., Connick,M. and Ames,B.N. (1983) Complete analysis of tRNA-modified nucleosides by high performance liquid chromatography: the 29 modified nucleosides of *Salmonella typhimurium* and *Escherichia coli*. *Anal. Biochem.*, **129**, 1–13.
36. Milligan,J.F., Groebe,D.R., Witherell,G.W. and Uhlenbeck,O.C. (1987) Oligoribonucleotide synthesis using T7 RNA polymerase and synthetic DNA templates. *Nucleic Acids Res.*, **15**, 8783–8798.
37. Bartosik,K. and Leszczynska,G. (2015) Synthesis of various substituted 5-methyluridines (xm5U) and 2-thiouridines (xm5s2U) via nucleophilic substitution of 5-pivaloyloxymethyluridine/2-thiouridine. *Tetrahedron Lett.*, **56**, 6593–6597.
38. Freibert,S.-A., Weiler,B.D., Bill,E., Pierik,A.J., Mühlenhoff,U. and Lill,R. (2018) Biochemical reconstitution and spectroscopic analysis of iron–sulfur proteins. *Methods Enzymol.*, **599**, 197–226.
39. Bouvier,D., Labessan,N., Clemancey,M., Latour,J.M., Ravanat,J.L., Fontecave,M. and Atta,M. (2014) TtcA a new tRNA-thioltransferase with an Fe-S cluster. *Nucleic Acids Res.*, **42**, 7960–7970.
40. Chen,M., Asai,S.I., Narai,S., Nambu,S., Omura,N., Sakaguchi,Y., Suzuki,T., Ikeda-Saito,M., Watanabe,K., Yao,M. *et al.* (2017) Biochemical and structural characterization of oxygen-sensitive 2-thiouridine synthesis catalyzed by an iron-sulfur protein TtuA. *Proc. Natl. Acad. Sci. USA*, **114**, 4954–4959.
41. Arragain,S., Bimai,O., Legrand,P., Caillat,S., Ravanat,J.L., Touati,N., Binet,L., Atta,M., Fontecave,M. and Golinelli-Pimpaneau,B. (2017) Nonredox thiolation in tRNA occurring via sulfur activation by a [4Fe-4S] cluster. *Proc. Natl. Acad. Sci. USA*, **114**, 7355–7360.
42. Armengod,M.E., Moukadiri,I., Prado,S., Ruiz-Partida,R., Benitez-Paez,A., Villarroya,M., Lomas,R., Garzon,M.J., Martinez-Zamora,A., Meseguer,S. *et al.* (2012) Enzymology of tRNA modification in the bacterial MnmEG pathway. *Biochimie*, **94**, 1510–1520.
43. Shigi,N., Horitani,M., Miyauchi,K., Suzuki,T. and Kuroki,M. (2020) An ancient type of MnmA protein is an iron-sulfur cluster-dependent sulfurtransferase for tRNA anticodons. *RNA*, **26**, 240–250.
44. Hewitson,K.S., Ollagnier-de Choudens,S., Sanakis,Y., Shaw,N.M., Baldwin,J.E., Münck,E., Roach,P.L. and M.,F. (2002) The iron-sulfur center of biotin synthase: site-directed mutants. *J. Biol. Inorg. Chem.*, **1–2**, 83–93.

45. Bak,D.W. and Elliott,S.J. (2014) Alternative FeS cluster ligands: tuning redox potentials and chemistry. *Curr. Opin. Chem. Biol.*, **19**, 50–58.
46. Calzolai,L., Gorst,C.M., Zhao,Z.H., Teng,Q., Adams,M.W. and La Mar,G.N. (1995) 1H NMR investigation of the electronic and molecular structure of the four-iron cluster ferredoxin from the hyperthermophile *Pyrococcus furiosus*. Identification of Asp 14 as a cluster ligand in each of the four redox states. *Biochemistry*, **34**, 11373–11384.
47. Imai,T., Taguchi,K., Ogawara,Y., Ohmori,D., Yamakura,F., Ikezawa,H. and Urushiyama,A. (2001) Characterization and cloning of an extremely thermostable, *Pyrococcus furiosus*-type 4Fe ferredoxin from *Thermococcus profundus*. *J. Biochem.*, **130**, 649–655.
48. Muraki,N., Nomata,J., Ebata,K., Mizoguchi,T., Shiba,T., Tamiaki,H., Kurisu,G. and Fujita,Y. (2010) X-ray crystal structure of the light-independent protochlorophyllide reductase. *Nature*, **465**, 110–114.
49. Kondo,T., Nomata,J., Fujita,Y. and Itoh,S. (2011) EPR study of 1Asp-3Cys ligated 4Fe-4S iron-sulfur cluster in NB-protein (BchN-BchB) of a dark-operative protochlorophyllide reductase complex. *FEBS Lett.*, **585**, 214–218.
50. Gruner,I., Fradrich,C., Bottger,L.H., Trautwein,A.X., Jahn,D. and Hartig,E. (2011) Aspartate 141 is the fourth ligand of the oxygen-sensing $[4Fe\text{-}4S]^{2+}$ cluster of *Bacillus subtilis* transcriptional regulator Fnr. *J. Biol. Chem.*, **286**, 2017–2021.
51. Jiang,H., Zhang,X., Ai,C., Liu,Y., Liu,J., Qiu,G. and Zeng,J. (2008) Asp97 is a crucial residue involved in the ligation of the [Fe4S4] cluster of IscA from *Acidithiobacillus ferrooxidans*. *J. Microbiol. Biotechnol.*, **18**, 1070–1075.
52. Liu,Y., Vinyard,D.J., Reesbeck,M.E., Suzuki,T., Manakongtreecheep,K., Holland,P.L., Brudvig,G.W. and Söll,D. (2016) A [3Fe-4S] cluster is required for thiolation in archaea and eukaryotes. *Proc. Natl. Acad. Sci. USA*, **113**, 12703–12708.
53. Flint,D.H. and Allen,R.M. (1996) Iron-sulfur proteins with nonredox functions. *Chem. Rev.*, **96**, 2315–2334.
54. Shigi,N. (2018) Recent advances in our understanding of the biosynthesis of sulfur modifications in tRNAs. *Front. Microbiol*, **9**, 2679.
55. Chen,M., Ishizaka,M., Narai,S., Horitani,M., Shigi,N., Yao,M. and Tanaka,Y. (2020) The [4Fe-4S] cluster of sulfurtransferase TtuA desulfurizes TtuB during tRNA modification in *Thermus thermophilus*. *Commun Biol*, **3**, 168.
56. Zhou,J., Pecqueur,L., Aučynaitė,A., Fuchs,J., Rutkienė,R., Vaitekūnas,J., Meškys,R., Boll,M., Fontecave,M., Urbonavičius,J. *et al.* (2021) Structural evidence for a [4Fe-5S] intermediate in the non-redox desulfuration of thiouracil. *Angew. Chem. Int. Ed. Engl.*, **60**, 424–431.
57. Beinert,H., Kennedy,M.C. and Stout,C.D. (1996) Aconitase as iron-sulfur protein, enzyme, and iron-regulatory protein. *Chem. Rev.*, **96**, 2335–2374.
58. Mulliez,E., Ollagnier-de Choudens,S., Meier,C., Cremonini,M., Luchinat,C., Trautwein,A.X. and Fontecave,M. (1999) Iron-sulfur interconversions in the anaerobic ribonucleotide reductase from *Escherichia coli*. *J. Biol. Inorg. Chem.*, **4**, 614–620.
59. Bühning,M., Valleriani,A. and Leimkühler,S. (2017) The role of SufS is restricted to Fe-S cluster biosynthesis in *Escherichia coli*. *Biochemistry*, **56**, 1987–2000.